BRAIN CONNECTIVITY
Volume 6, Number 3, 2016

DOI: 10.1089/brain.2015.0387

Plasticity of Interhemispheric Temporal Lobe White Matter Pathways Due to Early Disruption of Corpus Callosum Development in Spina Bifida

Kailyn A. Bradley,[1,2] Jenifer Juranek,[3] Anna Romanowska-Pawliczek,[3] H. Julia Hannay,[1] Paul T. Cirino,[1] Maureen Dennis,[4] Larry A. Kramer,[5] and Jack M. Fletcher[1]

Abstract

Spina bifida myelomeningocele (SBM) is commonly associated with anomalous development of the corpus callosum (CC) because of congenital partial hypogenesis and hydrocephalus-related hypoplasia. It represents a model disorder to examine the effects of early disruption of CC neurodevelopment and the plasticity of interhemispheric white matter connections. Diffusion tensor imaging was acquired on 76 individuals with SBM and 27 typically developing individuals, aged 8–36 years. Probabilistic tractography was used to isolate the interhemispheric connections between the posterior superior temporal lobes, which typically traverse the posterior third of the CC. Early disruption of CC development resulted in restructuring of interhemispheric connections through alternate commissures, particularly the anterior commissure (AC). These rerouted fibers were present in people with SBM and both CC hypoplasia and hypogenesis. In addition, microstructural integrity was reduced in the interhemispheric temporal tract in people with SBM, indexed by lower fractional anisotropy, axial diffusivity, and higher radial diffusivity. Interhemispheric temporal tract volume was positively correlated with total volume of the CC, such that more severe underdevelopment of the CC was associated with fewer connections between the posterior temporal lobes. Therefore, both the macrostructure and microstructure of this interhemispheric tract were reduced, presumably as a result of more extensive CC malformation. The current findings suggest that early disruption in CC development reroutes interhemispheric temporal fibers through both the AC and more anterior sections of the CC in support of persistent hypotheses that the AC may serve a compensatory function in atypical CC development.

Key words: corpus callosum; diffusion tensor imaging; fiber tracking; neural plasticity; temporal lobe

Introduction

Plasticity of interhemispheric connections has been hypothesized in people with congenital absence or partial development (hypogenesis) of the corpus callosum (CC). Full disconnection syndromes are rare in CC hypogenesis, with speculation that partially preserved interhemispheric transfer occurs through rerouted connections that traverse other commissures (Hannay et al., 2009; Paul, 2011). These hypotheses frequently invoke the anterior commissure (AC) or hippocampal commissure (Barkovich and Raybaud, 2012; Hannay et al., 2009), but little is known about these and other plastic connections in congenital disorders affecting the CC.

Diffusion tensor imaging (DTI) and tractography methods have made it possible to examine the structure of the CC and identify various atypical white matter connections. Crawley et al. (2014) used DTI and deterministic tractography to segment the CC in individuals with thinning of the CC due to hydrocephalus in spina bifida and found that posterior sections had the greatest reductions in volume and microstructural integrity. In addition, Probst bundles, which are anomalous, anterior-posterior coursing connections, as well as interhemispheric sigmoid-shaped bundles connecting heterotopic cortical regions, have been identified in individuals with congenital disorders affecting CC development (Barkovich and Raybaud, 2012; Lee et al.,

[1]Department of Psychology, University of Houston, Houston, Texas.
[2]Department of Psychiatry, Icahn School of Medicine at Mount Sinai, New York, New York.
[3]Department of Pediatrics, Children's Learning Institute, University of Texas Health Science Center at Houston, Houston, Texas.
[4]Program in Neurosciences and Mental Health, The Hospital for Sick Children, Toronto, Canada.
[5]Department of Diagnostic and Interventional Radiology, University of Texas Health Science Center at Houston, Houston, Texas.

2004; Owen et al., 2013; Tovar-Moll et al., 2007, 2014; Wahl et al., 2009).

Few studies have used probabilistic tractography to examine plastic connections between homotopic cortical regions in individuals with CC malformations. Tovar-Moll et al. (2014) recently found atypical white matter tracts connecting the posterior parietal cortices through both the anterior and posterior commissures in six individuals with partial or complete hypogenesis of the CC. However, conclusions from this small sample with little variation in CC dysmorphology are limited. Larger studies examining interhemispheric connections across diverse samples are needed to better understand the range of plastic connections that emerge due to CC maldevelopment.

Spina bifida myelomeningocele (SBM) is associated with both partial hypogenesis of the CC and hydrocephalus-related thinning or underdevelopment of the CC (hypoplasia), representing a unique population for investigation of how diverse and early CC malformations induce plasticity of interhemispheric white matter tracts (Dennis et al., 2006; Hannay et al., 2009). Hypogenesis of the posterior CC can be identified in about one-third to half of people with SBM, depending on resolution of the magnetic resonance imaging (MRI) (Juranek and Salman, 2010). Converging evidence suggests that posterior brain regions are especially anomalous in SBM (Juranek et al., 2008; Treble et al., 2013), but little is known about the interhemispheric connectivity of these regions. We used DTI and probabilistic tractography to qualitatively and quantitatively describe the organization, microstructure, and macrostructure of interhemispheric white matter connections between the posterior temporal lobes in a large sample of people with SBM relative to typically developing (TD) controls. We hypothesized the following:

1. Maldevelopment of the CC in SBM would reroute interhemispheric temporal lobe connections from the posterior CC to alternate commissures, with more severe CC hypogenesis associated with the most anomalous connectivity.
2. Reduced microstructural integrity—indexed by lower fractional anisotropy (FA), axial diffusivity (AD), and increased radial diffusivity (RD)—and decreased volume of the interhemispheric temporal tract in SBM, with CC hypogenesis associated with greater reductions in integrity.

Materials and Methods

Participants

Participants included 76 individuals with SBM and 27 TD comparisons, aged 8–36 years. Participants were recruited from the Spina Bifida Clinics at Texas Children's Hospital, the Shriner's Hospital for Children, and through advertisement from the community. Institutional Review Boards at The University of Houston and The University of Texas Health Science Center-Houston approved the protocol. Adolescents aged 13 and older and adults gave written informed consent. Children under 13 assented to the study. Parents of all participants under 18 gave written informed consent for participation.

General exclusionary criteria included the presence of other genetic, neurodevelopmental, or psychiatric disorders, and an uncontrolled seizure disorder. The TD group was solely right handed, but handedness was not controlled in the group with SBM because early brain injury often results in nonright-handedness and is a consequence of the injury (Fletcher et al., 2005). Table 1 contains participant demographics, showing differences in handedness, as well as lower SES and IQ scores in the group with SBM, which is a common finding in this population (Fletcher et al., 2005). There were no significant differences in age, sex, or ethnicity.

A representative sample of people with SBM, the majority had lower-level (<T1) spinal lesions (83%) and Type II Chiari malformations (86%). Seventy-five percent had hypoplastic CCs, with 21% showing more severe hypogenesis of the splenium. Most individuals (86%) were shunted for hydrocephalus.

Table 1. Demographic Information

	TD, n = *27; total sample*	*SBM,* n = *76; total sample*	*SBM CC hypoplastic,* n = *57 (75% of sample with SBM)*	*SBM CC hypogenesis,* n = *16 (21% of sample with SBM)*	*SBM CC intact,* n = *3 (4% of sample with SBM)*[a]
Age in years: M (SD)	16.96 (9.05)	14.56 (5.80)	14.86 (6.04)	13.07 (3.51)	16.75 (11.06)
Sex: *n* (% male)	13 (48.10)	39 (51.30)	29 (50.88)	9 (56.25)	1 (33.33)
SES: M (SD)[b]	40.98 (10.33)	32.13 (12.45)*	31.68 (11.53)	34.73 (16.05)	27.67 (11.37)
Handedness: *n* (% R)	27 (100.00)	62 (81.60)*	46 (80.70)	13 (81.25)	3 (100.00)
Ethnicity[c]					
Hispanic, *n* (%)	13 (48.10)	39 (51.30)	29 (50.88)	8 (50.00)	2 (66.67)
Non-Hispanic, *n* (%)	14 (51.90)	31 (40.80)	22 (38.60)	8 (50.00)	1 (33.33)
Stanford Binet IQ					
Verbal: M (SD)	99.78 (12.87)	84.76 (16.47)*	83.37 (16.51)	85.75 (15.49)	106.00 (2.00)
Nonverbal: M (SD)	105.19 (14.96)	90.08 (14.74)*	88.21 (13.46)	95.38 (17.03)	97.33 (22.30)

[a]Excluded from all statistical analyses due to small sample size ($n = 3$; 4% of the sample with SBM).
[b]Missing data on one participant.
[c]Missing data on six participants with SBM; percentages may not add to 100 due to missing data.
*$p < 0.05$ compared to the TD group.
CC, corpus callosum; SBM, spina bifida myelomeningocele; SES, socioeconomic status; TD, typically developing.

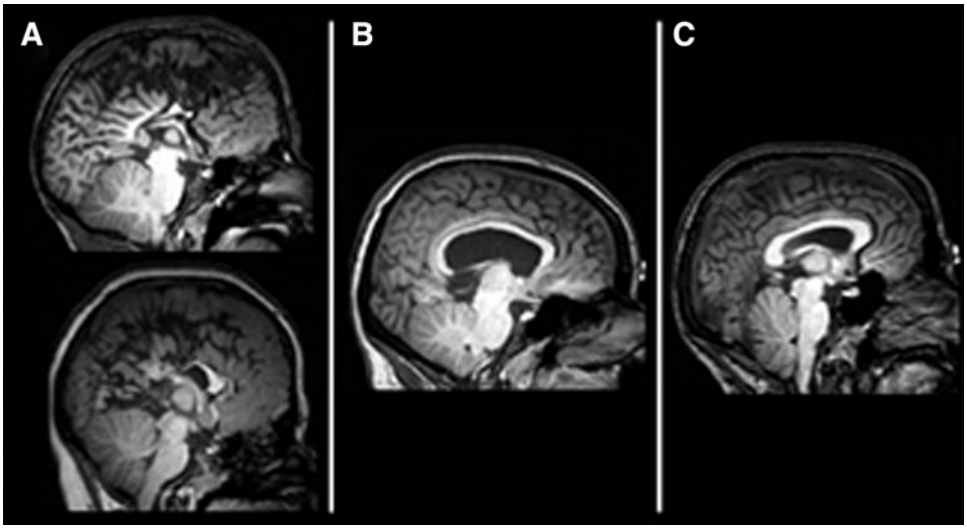

FIG. 1. Classification of the posterior CC in SBM. **(A)** *Top*: Hypogenesis of the CC with missing rostrum; *Bottom:* Hypogenesis of the CC with rostrum present; **(B)** Hypoplastic CC; **(C)** Intact/normal appearing CC. CC, corpus callosum; SBM, spina bifida myelomeningocele.

MRI data acquisition

MR images were acquired between 2005 and 2009 using a single 3 Tesla (T) Philips Intera scanner with SENSE (Sensitivity Encoding) technology. A stable acquisition protocol was utilized during the entire data collection period. High-resolution T_1-weighted anatomical images were acquired in the coronal plane using a 3D turbo fast echo sequence with the following parameters: voxel dimensions = 0.94×0.94 mm, slice thickness = 1.5 mm, repetition time (TR) = 6.50–6.70 msec, echo time (TE) = 3.04–3.14 msec, flip angle = 8°, diameter field of view (DFOV) = 240 mm, and matrix = 256×256. DTI images were acquired in the axial plane using a spin-echo diffusion sensitized echo-planar imaging sequence. Diffusion sensitizing gradients were applied in 21 directions (weighting: $b = 1000$ sec/mm^2) with one reference image ($b = 0$ sec/mm^2) and the following parameters: voxel dimensions = 0.94×0.94 mm, slice thickness = 3 mm, TR = 6500 msec, TE = 65 msec, flip angle = 90°, DFOV = 240 mm, and matrix = 256×256.

MRI data processing

Radiological coding of T_1-weighted images. T_1-weighted data of each participant were rated by a radiologist blind to the status of participants for qualitative classification of the entire CC, as well as the rostrum, genu, body, and splenium as present, absent, or hypoplastic. This assessment was based largely on the midsagittal slice, but other planes of view were available to the rater. If any subregion of the CC was rated as hypoplastic, the degree of thinning was rated as mild, moderate, or severe. The CCs of all TD participants were read as grossly intact and normal. However, there were a variety of CC dysmorphologies in people with SBM. These evaluations were used to classify people with SBM into three subgroups.

Hypogenesis subgroup: The most severe underdevelopment of the CC where the splenium was rated as absent or severely shortened and hypoplastic ($n = 16$; 21% of the sample with SBM; Fig. 1A).

Hypoplastic subgroup: Less severe disruption in CC development, with the splenium rated as present and only mildly or moderately thinned ($n = 57$; 75% of the sample with SBM; Fig. 1B).

Intact subgroup: All four subdivisions of the CC were rated as present and normal appearing ($n = 3$; 4% of the sample with SBM; Fig. 1C). These three participants were excluded from all statistical analyses due to the small sample size and are reported only for descriptive purposes.

Cortical parcellation of T_1-weighted images. Using FreeSurfer software, version 4.0.5 (www.surfer.nmr.mgh.harvard.edu), T_1-images were skull stripped and brain tissue segmented into gray or white matter and cerebrospinal fluid (CSF), and then parcellated into cortical regions of interest according to the Desikan and Destrieux Atlases (Fischl et al., 2002, 2004). Both the T_1-weighted image and cortical parcellation masks were transformed into diffusion space to be used for probabilistic tractography. Specifically, the linear transformation tool (FLIRT) from FMRIB's Software Library (FSL) version 5.0.1 (Jenkinson et al., 2012; Smith et al., 2004; Woolrich et al., 2009) was used to coregister the T_1-weighted volume with the same individual's nondiffusion-weighted volume using an affine transformation matrix.

Seed regions for tractography. Two separate seed masks were manually created over single coronal slices in the left and right posterior temporal lobes where Heschl's gyrus and the superior temporal lobe meet. This location was isolated in each participant by loading the cortical gray and white matter parcellations of Heschl's gyrus and the superior temporal lobes on the diffusion FA color map (Fig. 2). Hand-drawn coronal regions of interest (ROIs) have been used successfully to isolate transcallosal fibers connecting the temporal cortices in previous tractography studies examining typical individuals (Dougherty et al., 2007; Northam et al., 2012). A single exclusion mask was drawn over the midbrain to avoid tracking the ascending and descending auditory pathways. Since the temporal callosal segment of the CC is difficult to track due to anterior–posterior and ventral–dorsal crossing fibers (Wakana et al., 2007; Westerhausen et al.,

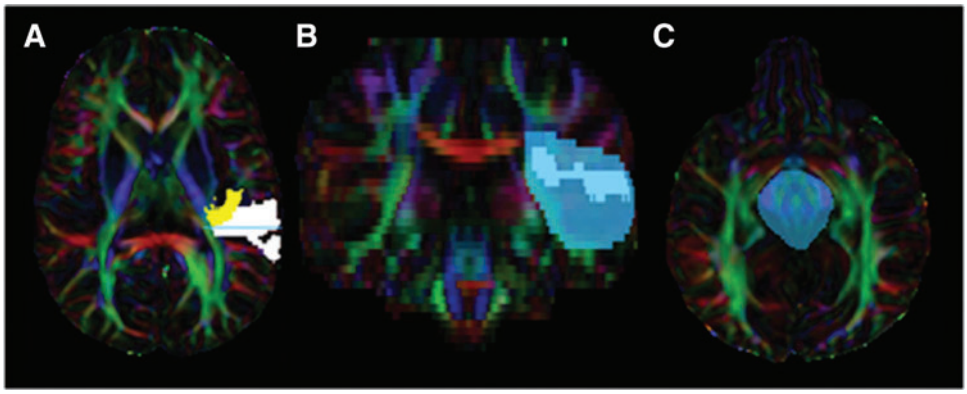

FIG. 2. Tractography ROI placement. Depiction of the posterior temporal lobe mask used in tractography. **(A)** Axial section showing the Heschl's gyrus ROI (*yellow*) and the posterior superior temporal lobe ROI (*white*) that were used as landmarks for placement of the posterior temporal lobe mask (*blue*) for tractography. **(B)** Coronal section showing that the posterior temporal lobe mask used for tractography (*blue*) overlapped Heschl's gyrus and the posterior superior temporal lobe ROIs. **(C)** Axial section showing the midbrain mask (*blue*) used to exclude the ascending and descending auditory pathways. ROI, region of interest. Color images available online at www.liebertpub.com/brain

2009), tractography seed masks included the tapetum—the white matter that runs along the lateral wall of the lateral ventricle and connects the temporal lobes through the posterior CC (Abe et al., 2004; Kim et al., 2008; Mori et al., 1999). In addition, the tapetum improves accuracy in isolating the interhemispheric temporal tract (Dougherty et al., 2007).

Intrarater reliability was evaluated for both the left and right hemisphere temporal lobe tractography seed masks through calculation of the Dice similarity coefficient. The mean Dice similarity coefficient of both the left and right seed masks in 10% of the sample selected at random was 0.93 (SD = 0.027). The Dice similarity coefficients ranged from 0.86 to 0.96, suggesting a very high level of intrarater reliability (Williams et al., 2013).

Seed-based probabilistic tractography. Diffusion tensor data were preprocessed for probabilistic tractography using FSL version 5.0.1 (Jenkinson et al., 2012; Smith et al., 2004; Woolrich et al., 2009). Images underwent a quality assurance protocol that evaluated motion and corrected for eddy current distortions. The nondiffusion-weighted volume ($b = 0\,\text{sec/mm}^2$) was skull stripped to create a brain mask using the brain extraction toolbox (Smith, 2002). Tensors were reconstructed using DTIFIT to generate FA, AD, and RD maps (Behrens et al., 2003). To ensure that tractography only occurred within brain tissue, the FA map underwent erosion with a three-dimensional kernel $3 \times 3 \times 3$. Additional processing with FSLs BEDPOSTX prepared the data for probabilistic fiber tracking (Behrens et al., 2003).

Two fiber tracts were created using FSLs PROBTRACKX. The first tract was seeded from the left posterior temporal lobe to the right posterior temporal lobe as a waypoint. The second tract was seeded from the right posterior temporal lobe to the left posterior temporal lobe as a waypoint. An exclusion mask of the midbrain was included in both tracts. The two reverse tracks were combined through FSL terminal commands that multiplied the binarized tracts together to only keep voxels that were shared between them; this method is equivalent to a logical AND such that voxels in the final tract must be present in both the reverse tracts. All DTI metrics were extracted from this combined tract to ensure that the most stringent criteria for selecting voxels that exist along the true white matter path were met (Javad et al., 2014; Jones, 2011).

A total of 5000 streamlines were sent out from each voxel in the seed ROI, with a step length of 0.5 mm and a curvature threshold of 0.2 ($\sim 80°$). The tracts were not restricted to travel through the CC to examine all potential interhemispheric connections between the auditory processing regions in the posterior temporal lobes. Final tract outputs were waytotal normalized; individual tract probabilities for each participant were calculated by dividing the probability density function for each voxel in the tract by the waytotal. A standardized probability threshold of 0.02 was applied to exclude extraneous fibers. To accommodate reduced FA due to CC maldevelopment (Wahl et al., 2009), tracts were further restricted by retaining voxels with FA values between 0.15 and 1.0. Final tracts were binarized and mean FA, AD, and RD were obtained through FSL terminal commands. The entire process of computations was fully automated through the use of bash scripts executing FSL commands. A qualitative examination of the tracts viewed over both coregistered T_1-weighted volumes and DTI FA maps determined the location of decussation of the interhemispheric temporal fibers.

Calculation of total CC tract volume. A measure of total CC tract volume was obtained to quantitatively assess the degree of CC underdevelopment. Given that qualitative classification of CC hypoplasia and hypogenesis is not always clear in the highly dysmorphic SBM brain, a quantitative measure of total CC tract volume may better elucidate the relation between CC morphology and interhemispheric temporal tract microstructure and macrostructure. This quantitative measure of total CC tract volume was obtained using deterministic tractography. Fiber tracking of the total CC was performed with the fiber assignment by continuous tracking (FACT) algorithm in TrackVis (http://trackvis.org), whereby the CC tract was seeded by all white matter voxels in the brain, keeping only those fibers that crossed through a manually drawn ROI of the CC (Wahl et al., 2009;

Weeden et al., 2008). The ROI consisted of the centermost midsagittal slice of the CC as well as three slices to the left and three slices to the right of the center to get good three-dimensional coverage of the CC. The CC tract volume was obtained through TrackVis statistics. Volume of the entire CC tract was normalized by total white matter in the brain and multiplied by 100 to get the percentage of white matter in the brain that the CC encompasses. Previous work (Juranek et al., 2008) has shown that compared to TD individuals, those with SBM show a 15% reduction in total white matter in the brain, but not gray matter. Therefore, it is necessary to account for this between group variability when comparing volumes of a single white matter tract of interest to get an accurate estimation of group differences specifically in that tract.

Statistical analyses

Both qualitative and quantitative measures were used to describe interhemispheric connectivity between the temporal lobes in TD individuals and two subgroups with SBM (i.e., CC hypogenesis and hypoplasia). To reiterate, individuals with SBM and an intact normal appearing CC were excluded from all statistical analyses due to the small sample size ($n=3$; 4% of the sample with SBM). Qualitative ratings of the location of interhemispheric temporal lobe connections were made and patterns of connectivity were compared between the TD and SBM subgroups using chi-square tests or Fisher's exact tests where appropriate. Comparisons were also made between two subgroups with SBM based on CC dysmorphology (i.e., CC hypogenesis and hypoplasia; Hypothesis 1).

To examine the possible relation between CC morphology and DTI microstructure (i.e., FA, AD, and RD) and macrostructure (i.e., volume) of the interhemispheric temporal tract, both categorical and dimensional analyses were employed (Hypothesis 2). Analysis of covariance (ANCOVA) with age as a covariate evaluated differences between three groups (i.e., TD, SBM CC hypoplasia, and SBM CC hypogenesis) in FA, AD, and RD. Similarly, ANCOVA with age as a covariate evaluated group differences in tract macrostructure (i.e., volume). All *post hoc* pairwise comparisons controlled the family-wise error rate using a conservative Bonferroni correction ($\alpha=0.05/3=0.0167$). A dimensional approach was additionally used to investigate the relations of CC morphology and DTI microstructure and macrostructure within the group with SBM; partial correlations controlling for age assessed the associations between DTI microstructure (i.e., FA, AD, and RD) and macrostructure (i.e., volume) of the interhemispheric temporal tract. Statistical significance was defined as two-tailed with $p<0.05$.

Results

Location of interhemispheric temporal connections

TD and SBM group differences. Tractography results demonstrated that all 27 participants in the TD group displayed the normative pattern of connection between the posterior temporal lobes through the posterior third of the CC (i.e., splenium and isthmus as illustrated in Fig. 3). However, in the group with SBM, seven patterns of interhemispheric connection were observed (Fig. 4).

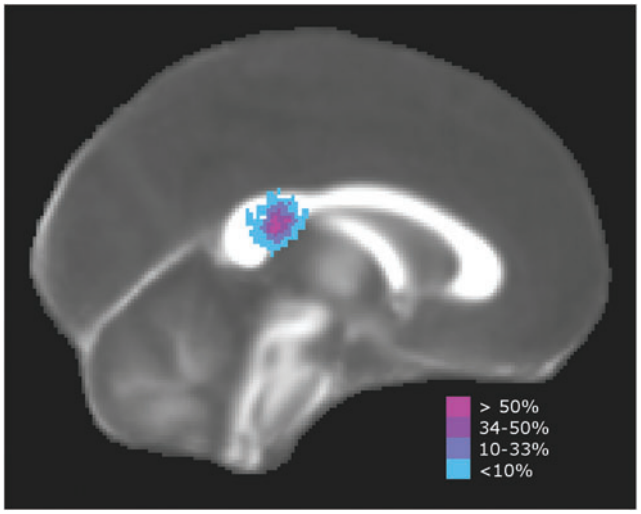

FIG. 3. Interhemispheric temporal tracts in the TD group. Standard space template showing the percentage of TD participants ($n=27$) with tracts crossing through the posterior CC. TD, typically developing. Color images available online at www.liebertpub.com/brain

Fifty-two percent of the group with SBM displayed the typical pattern of connection through the posterior third of the CC. However, 25% had connections through both the posterior CC and the AC, and in 13% of the sample, connections traversed only the AC—no visible tracts crossed through the CC. Four additional patterns of interhemispheric connection occurred less frequently (<10%) in the group with SBM. Two participants had connections through a more anterior section of the CC and the AC, and two others had connections through a very small callosal remnant and the AC. One participant had connections through both the anterior and posterior CC, and another had connections through the anterior CC, posterior CC, and the AC (Fig. 4).

Fisher's exact test showed that the proportion of individuals with typical posterior CC connectivity compared to altered connectivity differed significantly between the TD group and the group with SBM ($p<0.0005$). As hypothesized, the group with SBM had a greater number of individuals with alternative interhemispheric temporal pathways (48% in SBM vs. 0% in TD).

CC dysmorphology in SBM. Table 2 displays tractography results for subgroups with SBM: intact CC, CC hypoplasia, and CC hypogenesis. Although excluded from statistical analyses because of the infrequency of a normal appearing CC in the group with SBM, note that two out of the three participants identified with an intact CC in the group with SBM had connections through both the posterior CC and the AC. This pattern was not seen in any individuals in the TD group.

A chi-square test of independence comparing two subgroups with SBM, one with CC hypoplasia and the other with CC hypogenesis on patterns of posterior CC connectivity was significant, $\chi^2=4.44$, $p=0.035$. The group with SBM and CC hypoplasia had more people with the normative pattern of posterior CC connection (86%) than those with more severe CC hypogenesis (63%). In addition, there was no significant difference in the frequency of AC connectivity between individuals with SBM and CC hypoplasia or hypogenesis, $\chi^2=1.01$, $p=0.32$.

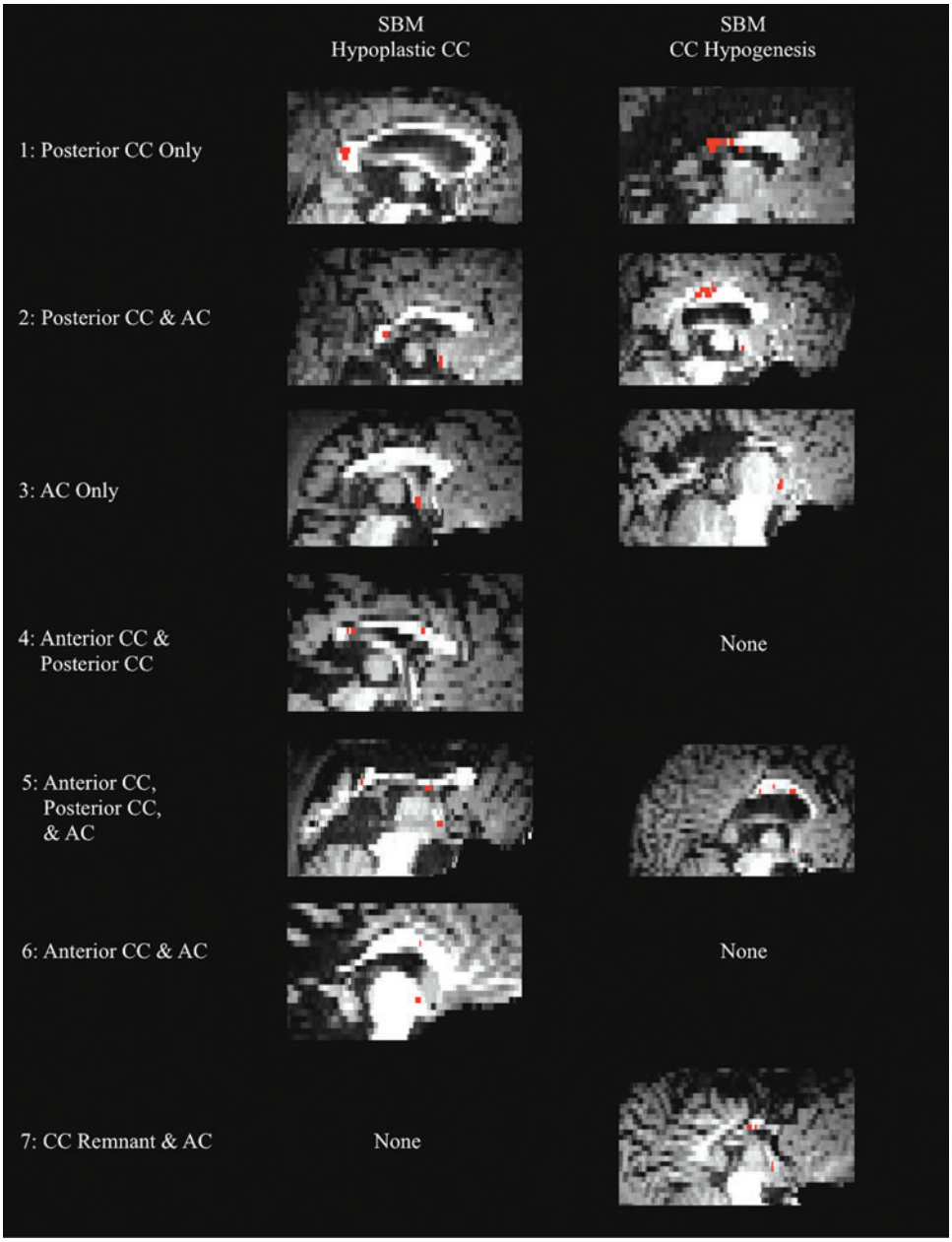

FIG. 4. Interhemispheric temporal tracts in SBM. Midsagittal T1-weighted images coregistered to diffusion space of the seven different interhemispheric tract patterns present in participants with SBM. The *left column* of images shows patterns present in individuals with SBM and CC hypoplasia. The *right column* shows patterns present in individuals with SBM and CC hypogenesis. AC, anterior commissure; *Red*, interhemispheric temporal tract. Color images available online at www.liebertpub.com/brain

Given the number of individuals with SBM and connection through the AC, several exploratory follow-up analyses were conducted. A univariate 2×2 ANOVA examined the interaction between CC dysmorphology (i.e., CC hypoplasia or hypogenesis) and AC intersection (i.e., crosses the AC or not) on the cross-sectional area of the AC. The cross-sectional area of the AC was quantified through measurements of the AC taken in two planes. The interaction of CC dysmorphology and AC intersection was not significant, $F(1, 69) = 1.62$, $p = 0.21$. However, there was a main effect of CC dysmorphology; individuals with SBM and CC hypoplasia had larger ACs ($M = 10.88$, $SD = 6.59$) than those with SBM and CC hypogenesis ($M = 7.14$, $SD = 3.28$), $F(1, 71) = 4.94$, $p = 0.03$, partial $\eta^2 = 0.07$.

In addition, a univariate one-way ANOVA examined cross-sectional area of the AC in individuals with SBM and connections through the AC compared to those without AC tracts, irrespective of CC dysmorphology. Individuals with SBM and tracts that crossed through the AC had a larger cross-sectional area of the AC ($M = 12.05\,mm^2$, $SD = 6.99$) compared to those that did not ($M = 8.42\,mm^2$, $SD = 4.78$), $F(1,71) = 6.87$, $p = 0.01$, partial $\eta^2 = 0.09$.

Microstructure and macrostructure of interhemispheric connections

TD and SBM group differences. Group means and standard deviations for FA, AD, RD, and volume of the interhemispheric temporal tract are presented in Table 3.

Fractional anisotropy: There was a significant main effect of group, $F(2,96) = 24.41$, $p < 0.0005$, partial $\eta^2 = 0.34$, with higher FA values in the TD group than both groups with SBM ($p < 0.0005$). However, the two groups with SBM were

Table 2. Interhemispheric Connections Between the Posterior Temporal Lobes in SBM (*N* [%])

Location	*SBM CC intact,* n = *3 (4% of sample with SBM)*[a]	*SBM CC hypoplastic,* n = *57 (75% of sample with SBM)*	*SBM CC hypogenesis,* n = *16 (21% of sample with SBM)*	*SBM total sample* n = *76*
1 Posterior CC	1 (33)	32 (56)	7 (44)	40 (53)
2 Posterior CC and AC	2 (67)	15 (26)	2 (13)	19 (25)
3 AC only	0	6 (11)	4 (25)	10 (13)
4 Anterior and posterior CC	0	1 (2)	0	1 (1)
5 AC, anterior CC, and posterior CC	0	1 (2)	1 (6)	2 (3)
6 Anterior CC and AC	0	2 (4)	0	2 (3)
7 CC remnant and AC	0	0	2 (13)	2 (3)

Percentages may not add up to 100% due to rounding.
[a]Excluded from all statistical analyses due to small sample size ($n = 3$; 4% of the sample with SBM).
AC, anterior commissure.

not significantly different from one another ($p = 0.19$). Age approached significance in the ANCOVA model and was therefore retained ($p = 0.05$). Age was weakly positively correlated with FA across both groups ($n = 100$; $\rho = 0.19$, $p = 0.06$) and in the group with SBM ($n = 73$; $\rho = 0.23$, $p = 0.05$), but not in the TD group ($n = 27$; $\rho = 0.09$, $p = 0.67$).

Axial diffusivity: There was no significant effect of age ($p > 0.05$), so it was trimmed form the model. There was a significant main effect of group, $F(2,97) = 7.16$, $p = 0.001$, partial $\eta^2 = 0.13$, with higher AD values in the TD group compared to both groups with SBM ($p < 0.005$). However, the two groups with SBM were not significantly different ($p = 0.94$).

Radial diffusivity: Age was trimmed due to no significant effect ($p > 0.05$). There was a significant main effect of group, $F(2,97) = 7.87$, $p = 0.001$, partial $\eta^2 = 0.14$, with higher RD in both groups with SBM compared to TD individuals ($p < 0.003$). However, the two groups with SBM were not significantly different ($p = 0.89$).

Tract volume: Age was not a significant effect ($p > 0.05$), so it was trimmed from the model. There were no significant group differences in interhemispheric tract volume, $F(2,97) = 2.71$, $p = 0.07$, partial $\eta^2 = 0.05$.

Quantitative measure of CC morphology in SBM. In addition to comparing qualitative subgroups of individuals with SBM and either CC hypoplasia or hypogenesis, a dimensional approach was also used to better evaluate the relation between CC morphology and interhemispheric tract integrity in SBM. A quantitative measure of total CC volume relative to the size of the brain was used (see Calculation of total CC tract volume in Materials and Methods section) as a continuous variable representing CC morphology. The entire CC was 7.49% of the white matter volume in the TD group, while it was only 5.60% in the group with SBM and CC hypoplasia and 2.96% in the group with SBM and CC hypogenesis. An ANCOVA, controlling for age, showed a main effect of group, $F(2,96) = 70.63$, $p < 0.0005$, partial $\eta^2 = 0.60$, with pairwise comparisons of all three groups significantly different in total volume of the CC ($p < 0.0005$). Partial correlations controlling for age assessed the relationship between CC morphology as quantified by total CC volume and interhemispheric tract microstructure in the group with SBM ($n = 76$).

Fractional anisotropy: The positive correlation between interhemispheric temporal tract FA and total CC volume was significant, $r = 0.38$, $p = 0.001$. Increased CC volume was associated with increased interhemispheric temporal tract FA.

Axial diffusivity: The positive correlation between interhemispheric temporal tract AD and total CC volume failed to reach statistical significance, $r = 0.12$, $p = 0.32$.

Radial diffusivity: The negative correlation between interhemispheric temporal tract RD and total CC volume was

Table 3. DTI Metrics

	TD, n = *27 (100% of sample)*	*SBM CC intact,* n = *3 (4% of sample with SBM)*[a]	*SBM CC hypoplastic,* n = *57 (75% of sample with SBM)*	*SBM CC hypogenesis,* n = *16 (21% of sample with SBM)*	p	*Contrasts*
FA	0.566 (0.048)	0.472 (0.138)	0.460 (0.081)	0.418 (0.069)	<0.0005*	TD > HP; TD > HG
AD[b]	1.70 (0.097)	1.51 (0.073)	1.59 (0.143)	1.55 (0.187)	0.001*	TD > HP; TD > HG
RD[b]	0.639 (0.104)	0.706 (0.192)	0.769 (0.174)	0.817 (0.198)	0.001*	HP > TD; HG > TD
Volume[c]	2305.09 (512.22)	1871.46 (224.24)	2441.11 (929.32)	1906.91 (765.40)	0.07	

[a]Excluded from all statistical analyses due to small sample size ($n = 3$; 4% of the sample with SBM).
[b]Units = $\times 10^{-3}$ mm^2/sec.
[c]Units = mm^3.
*Indicates significant group differences, $p < 0.05$.
AD, axial diffusivity; FA, fractional anisotropy; HG, CC hypogenesis; HP, hypoplastic CC; RD, radial diffusivity.

marginally significant, $r = -0.23$, $p = 0.05$. Decreased CC volume was associated with increased interhemispheric temporal tract RD.

Tract volume: The positive correlation between total CC volume and interhemispheric temporal tract volume was marginally significant, $r = 0.22$, $p = 0.056$. Increased CC volume was associated with increased volume of the interhemispheric temporal tract.

Discussion

Plastic reorganization of interhemispheric white matter due to early disruption in CC development is not well understood. No studies to date have utilized samples of sufficient size to comprehensively examine the relations of CC hypoplasia, CC hypogenesis, and interhemispheric temporal tract macrostructure and microstructure in any neurodevelopmental disorder. The key findings were that early disruption in the development of CC resulted in plasticity of interhemispheric connections between the posterior temporal lobes and rerouting through alternate commissures. These rerouted fibers traversed through the AC, as well as more anterior sections of the CC, and were present in individuals with SBM and both CC hypoplasia and more severe CC hypogenesis, but not the TD group. Both the microstructure and macrostructure of this interhemispheric temporal tract were reduced, especially in severe hypogenesis, presumably as a result of more extensive CC malformation.

Patterns of interhemispheric connection

We hypothesized that interhemispheric connections between the posterior temporal lobes would exist in people with CC hypoplasia and hypogenesis, but possibly through alternate commissures. Disconnection syndromes are rare in complete agenesis of the CC (Paul, 2011) and SBM (Hannay et al., 2008, 2009), which suggests that some mode of preserved cross-hemisphere communication exists despite underdevelopment of the CC. In support of this hypothesis, the group with SBM displayed seven different patterns of interhemispheric connection, six of which deviated from typical development. The normative pattern of connection between the superior temporal lobes should be through the posterior third of the CC—the splenium and isthmus (Westerhausen et al., 2009), which was found in the entire TD group ($n = 27$). However, only 53% of the group with SBM showed this pattern without additional anomalous connections through the AC or anterior regions of the CC.

Further investigation of this finding in the group with SBM revealed that the degree of CC maldevelopment (i.e., CC hypoplasia vs. hypogenesis), based on visual coding of scans, was not associated with the frequency of AC connections. However, CC hypoplasia was associated with a greater frequency of the typical pattern of posterior CC connectivity compared to CC hypogenesis. In addition, people with SBM and interhemispheric temporal connections through the AC had *larger* cross-sectional area measurements of the AC, with the subgroup with CC hypoplasia showing greater enlargement compared to those with CC hypogenesis. Therefore, while both subgroups with SBM had similar proportions of people with connections through the AC, and the AC was enlarged in those with aberrant AC connections, individuals with CC hypoplasia had greater enlargement and more variability in AC size compared to those with more severe hypogenesis. This finding was unexpected given that Hannay et al. (2009) found the AC enlarged in only 3% of a different sample of 193 people with SBM. The AC was classified as enlarged in Hannay's study based on the visual rating of a 1.5T T_1-weighted image and not a quantitative cross-sectional measurement of the AC. This new result demonstrates the added information that may be gained by using a higher field strength MRI scanner (i.e., 3T) for more detailed images. Conversely, previous investigations of AC size in other human and animal models support these findings. Individual case studies have shown AC enlargement in complete agenesis of the CC (Fischer et al., 1992), and studies of callosal agenesis in animal models suggest that the AC may be a common site of plastic reorganization of interhemispheric connections when the CC completely fails to form (Patel et al., 2010). Specifically, acallosal mice showed an increase in the total number of axons that traversed the AC (Livy et al., 1997).

Whether or not these aberrant AC connections are compensatory is still debated. Atypical performance on a dichotic listening task has been reported in people with CC hypogenesis, but not with CC hypoplasia (Hannay et al., 2009). Both subgroups with SBM and CC hypoplasia and more severe hypogenesis had a similar number of people with AC connections, suggesting these tracts may serve some level of compensatory function in both groups. However, preserved posterior CC connection, which was greater in the group with CC hypoplasia, may be most important to maintaining typical auditory function. A similar recent study of six individuals with complete or partial CC hypogenesis found that anomalous interhemispheric tracts between the parietal lobes traversed the anterior and posterior commissures and were associated with preserved transfer of tactile information for object recognition (Tovar-Moll et al., 2014). Therefore, while atypical, these interhemispheric connections through the AC may aid, to some degree, in the preservation of cognitive function.

Microstructure and macrostructure

We additionally hypothesized that maldevelopment of the CC would not only reroute interhemispheric fibers but also would result in reduced micro- and macrostructural integrity. In support of this hypothesis, we found that people with SBM and both CC hypoplasia and hypogenesis showed decreased FA and AD, and increased RD compared to the TD group. These results are supported by a previous investigation of CC microstructure that was restricted to CC hypoplasia in SBM, which showed reduced FA and increased RD in the entire CC, with posterior subregions showing the greatest reductions in integrity (Crawley et al., 2014).

Contrary to our hypothesis that more severe underdevelopment of the CC would be associated with the greatest reductions in integrity of the temporal tract, there were no differences between people with CC hypoplasia and hypogenesis in FA, AD, RD, or tract volume when subgroups were based on qualitative coding of scans. However, dimensional analyses that utilized a quantitative measure of total CC volume found a significant relation between CC dysmorphology and integrity of the interhemispheric temporal tract.

Reduced volume of the entire CC—representing more severe underdevelopment—was associated with increased RD, and lower FA and volume of the interhemispheric temporal tract. This is not surprising because dimensional approaches typically have more power. Thus, more severe underdevelopment of the CC due to early insult was associated with rerouted interhemispheric temporal tracts, as well as reductions in both microstructural and macrostructural integrity.

Research in healthy participants has shown that microstructural integrity of the interhemispheric temporal tract is correlated with performance on the dichotic listening task, which requires cross-hemisphere transfer of auditory information (Westerhausen et al., 2009). However, Crawley et al. (2014) found no relation between dichotic performance and CC microstructure in individuals with only mild CC thinning. Given that performance on the dichotic listening task, as well as other cognitive assessments, is typically most anomalous in people with severe CC hypogenesis, future studies should expand the current work to examine interhemispheric network function in the context of both microstructural and macrostructural level insults.

Limitations

Although these findings suggest that individuals with SBM exhibit abnormalities in interhemispheric tract microstructure, confounding partial volume effects cannot be ignored. The location of the interhemispheric temporal tract near the lateral ventricles, which are often enlarged in SBM, and the smaller size of the CC in SBM, could potentially increase the influence of partial volume effects from the surrounding tissues and CSF in this population (Voss et al., 2011). Previous studies have found that regional CC size measurements are correlated with diffusion parameters, such that smaller callosa are associated with lower FA and higher RD (Voss et al., 2011; Westerhausen et al., 2011). Similar results were found in this study; individuals with SBM had smaller interhemispheric temporal tracts with lower FA and higher RD. However, recent studies have shown that tracts further from the ventricles, such as parietal tectocortical pathways in SBM (Williams et al., 2013), also show a similar pattern of reduced microstructural integrity, supporting this conclusion in the current study. In addition, Williams et al. (2015) also found that increased ventricular volume in SBM was actually a predictor for the opposite pattern of increased FA and reduced RD in frontal and parietal tectocortical pathways. Therefore, it is likely that the group differences in microstructure that we document are not entirely due to the enlargement of ventricles in our patient sample and greater partial volume effects. Thus, there may be true microstructural degradation in the interhemispheric temporal tract in SBM, but the neurobiological inferences that can be drawn from these DTI measures warrant further investigation.

In addition, several other limitations of the DTI methodology should be noted. For example, confidence of tractography connections is decreased over large distances (Javad et al., 2014; Jones, 2011), and lower than ideal spatial resolution and DTI sensitivity may contribute to the ''crossing-fibers'' problem. Our slice thickness of 3 mm and 21 diffusion directions were not ideal, but represented the limit of our available technology, when the study was initiated in 2005, and the need to reduce scan time for younger children. The current method of combining only common fibers from two reverse tracts, each with a seed point in one hemisphere and a mandatory waypoint in the opposite hemisphere, along with an exclusion mask through the midbrain, helps minimize any inclusion of noninterhemispheric association tracts. Given that the tracts of interest were identified successfully in a large sample, higher spatial resolution studies are warranted. Newer imaging methods such as high angular-resolution diffusion imaging, which uses larger numbers of diffusion directions, may better isolate interhemispheric tracts (Shattuck et al., 2008; Tuch et al., 2002) and allow for more detailed investigations of interhemispheric tract structure, while minimizing partial volume effects as well as the intravoxel crossing-fibers problem. For example, these methods may be better able to isolate tracts that run through small structures such as the anterior and hippocampal commissures, which should be further investigated given the current findings.

Last, our groups were not matched on handedness, and nonright-handedness is more common in SBM than the general population (Fletcher et al., 2005). Since left-handedness has been associated with both larger (Westerhausen et al., 2004) and smaller (Witelson, 1985) midsagittal area of the CC, which can affect the susceptibility of the interhemispheric tract to partial volume effects, it cannot be entirely discounted as a confounding factor in the current investigation. At the same time, increased rates of nonright-handedness are a common consequence of early brain injury and control of handedness would limit the diversity of the sample.

Conclusion

Early disruption in CC development in SBM resulted in plastic reorganization of interhemispheric connections between the posterior temporal lobes. In addition, both microstructure and macrostructure of the interhemispheric temporal tract were associated with the severity of CC dysmorphology. This study was the first to our knowledge to examine the macrostructure and microstructure of the interhemispheric temporal tract in a large sample of people with both CC hypoplasia and hypogenesis. Because connections through alternative commissures such as the AC were found in people with both hypogenesis and hypoplasia of the CC, these findings have implications beyond just one etiology or one type of disruption in neurodevelopment. Given that there are many different causes of these CC anomalies outside of SBM (Anderson et al., 2001), this novel finding may extend to other genetic and neurodevelopmental disorders as well. Future research should specifically examine how these plastic connections relate to cognitive function as the degree of cognitive compensation gained by these connections is unknown. Newer imaging methodologies have the potential to further push the boundaries on examining the relation between plasticity and function in neurodevelopment.

Acknowledgments

This work was supported by the Eunice Kennedy Shriver National Institute of Child Health and Human Development grant P01-HD35946-06 (to J.M.F.). The content is solely the

responsibility of the authors and does not necessarily represent the official views of the Eunice Kennedy Shriver National Institute of Child Health and Human Development or the National Institutes of Health. Maureen Dennis passed away on July 14, 2014, but helped to design the study and interpret the results.

Author Disclosure Statement

No competing financial interests exist.

References

Abe O, Masutani Y, Aoki S, Yamasue H, Yamada H, Kasai K, et al. 2004. Topography of the human corpus callosum using diffusion tensor tractography. J Comput Assist Tomogr 28:533–539.

Anderson V, Northam E, Hendy J, Wrennall J. 2001. *Developmental Neuropsychology: A Clinical Approach*. New York, NY: Psychology Press.

Barkovich AJ, Raybaud C. 2012. *Pediatric Neuroimaging*. 5th ed. Philadelphia, PA: Lippincott Williams and Wilkins.

Behrens TE, Woolrich MW, Jenkinson M, Johansen-Berg H, Nunes RG, Clare S, et al. 2003. Characterization and propagation of uncertainty in diffusion-weighted MR imaging. Magn Reson Med 50:1077–1088.

Crawley J, Hasan K, Hannay HJ, Dennis M, Jockell C, Fletcher JM. 2014. Structure, integrity, and function of the hypoplastic corpus callosum in spina bifida myelomeningocele. Brain Connect 4:608–618.

Dennis M, Landry SH, Barnes M, Fletcher JM. 2006. A model of neurocognitive function in spina bifida over the life span. J Int Neuropsychol Soc 12:285–296.

Dougherty RF, Ben-Shachar M, Deutsch GK, Hernandez A, Fox GR, Wandell BA. 2007. Temporal-callosal pathway diffusivity predicts phonological skills in children. Proc Natl Acad Sci U S A 104:8556–8561.

Fischer M, Ryan SB, Dobyns WB. 1992. Mechanisms of interhemispheric transfer and patterns of cognitive function in acallosal patients of normal intelligence. Arch Neurol 49: 271–277.

Fischl B, Salat DH, Busa E, Albert M, Dieterich M, Haselgrove C, et al. 2002. Whole brain segmentation: automated labeling of neuroanatomical structures in the human brain. Neuron 33:341–355.

Fischl B, Salat DH, van der Kouwe A, Makris N, Segonne F, Quinn BT, et al. 2004. Sequence-independent segmentation of magnetic resonance images. Neuroimage 23(Supp 1):69–84.

Fletcher JM, Copeland K, Frederick JA, Blaser SE, Kramer LA, Northrup H, et al. 2005. Spinal lesion level in spina bifida: a source of neural and cognitive heterogeneity. J Neurosurg 3:268–279.

Hannay HJ, Dennis M, Kramer L, Blaser S, Fletcher JM. 2009. Partial agenesis of the corpus callosum in spina bifida meningomyelocele and potential compensatory mechanisms. J Clin Exp Neuropsychol 31:180–194.

Hannay HJ, Walker A, Dennis M, Kramer L, Blaser S, Fletcher JM. 2008. Auditory interhemispheric transfer in relation to patterns of partial agenesis and hypoplasia of the corpus callosum in spina bifida meningomyelocele. J Int Neuropsychol Soc 14:771–781.

Javad F, Warren JD, Micallef C, Thornton JS, Golay X, Yousry T, et al. 2014. Auditory tracts identified with combined fMRI and diffusion tractography. Neuroimage 84:562–574.

Jenkinson M, Beckman CF, Behrens TE, Woolrich MW, Smith SM. 2012. FSL. Neuroimage 62:782–790.

Jones DK. 2011. *Diffusion MRI: Theory, Methods and Applications*. New York, NY: Oxford University Press.

Juranek J, Fletcher JM, Hasan KM, Breier JI, Cirino PT, Pazo-Alvarez P, et al. 2008. Neocortical reorganization in spina bifida. Neuroimage 40:1516–1522.

Juranek J, Salman MS. 2010. Anomalous development of brain structure and function in spina bifida myelomeningocele. Dev Disabil Res Rev 16:23–30.

Kim H, Piao Z, Liu P, Bingaman W, Diehl B. 2008. Secondary white matter degeneration of the corpus callosum in patients with intractable temporal lobes epilepsy: a diffusion tensor imaging study. Epilepsy Res 81:136–142.

Lee S, Susumu M, Dong JK, Sei YK, Si YK, Dong IK. 2004. Diffusion tensor MR imaging visualizes the altered hemispheric fiber connection in callosal dysgenesis. ANJR Am J Neuroradiol 25:25–28.

Livy DJ, Schalomon PM, Roy M, Zacharias MC, Pimenta J, Lent R, Wahlsten D. 1997. Increased axon number in the anterior commissure of mice lacking a corpus callosum. Exp Neurol 146:491–501.

Mori S, Crain BJ, Chacko VP, van Zijl PCM. 1999. Three-dimensional tracking of axonal projections in the brain by magnetic resonance imaging. Ann Neurol 45:265–269.

Northam GB, Liegeois F, Tournier J, Croft LJ, Johns PN, Chong WK, et al. 2012. Interhemispheric temporal lobe connectivity predicts language impairment in adolescents born preterm. Brain 135:3781–3798.

Owen JP, Li YO, Ziv E, Strominger Z, Gold J, Bukhpun P, et al. 2013. The structural connectome of the human brain in agenesis of the corpus callosum. Neuroimage 70:340–355.

Patel M, Toussaint N, Charles-Edwards G, Lin J, Batchelor P. 2010. Distribution and fibre similarity mapping of the anterior commissure fibres by diffusion tensor imaging. MAGMA 23:399–408.

Paul LK. 2011. Developmental malformation of the corpus callosum: a review of typical callosal development and examples of developmental disorders with callosal involvement. J Neurodev Disord 3:3–27.

Shattuck DW, Chiang MC, Barysheva M, McMahon KL, de Zubicaray GI, Meredith M, et al. 2008. Visualization tools for high angular resolution diffusion imaging. Med Image Comput Comput Assist Interv 11:298–305.

Smith SM. 2002. Fast robust automated brain extraction. Hum Brain Mapp 17:143–155.

Smith SM, Jenkinson M, Woolrich MW, Beckman CF, Behrens TE, Johansen-Berg H, et al. 2004. Advances in functional and structural MR image analysis and implementation as FSL. Neuroimage 23:208–219.

Tovar-Moll F, Moll J, de Oliveira-Souza R, Bramati I, Andreiuolo PA, Lent R. 2007. Neuroplasticity in human callosal dysgenesis: a diffusion tensor imaging study. Cereb Cortex 17:531–541.

Tovar-Moll F, Monteiro M, Andrade J, Bramati IE, Vianna-Barbosa R, Marins T, et al. 2014. Structural and functional brain rewiring clarifies preserved interhemispheric transfer in humans born without the corpus callosum. Proc Natl Acad Sci U S A 111:7843–7848.

Treble A, Juranek J, Stuebing KK, Dennis M, Fletcher JM. 2013. Functional significance of atypical cortical organization in spina bifida myelomeningocele: relations of cortical thickness and gyrification with IQ and fine motor dexterity. Cereb Cortex 23:2357–2369.

Tuch DS, Reese TG, Wiegell MR, Makris N, Belliveau JW, Wedeen VJ. 2002. High angular resolution diffusion imaging reveals intravoxel white matter fiber heterogeneity. Magn Reson Med 48:577–582.

Voss SB, Jones DK, Viergever MA, Leemans A. 2011. Partial volume effect as a hidden covariate in DTI analyses. Neuroimage 55:1566–1576.

Wahl M, Strominger Z, Jeremy RJ, Barkovich AJ, Wakahiro M, Sherr EH, et al. 2009. Variability of homotopic and heterotopic callosal connectivity in partial agenesis of the corpus callosum: a 3T diffusion tensor imaging and Q-ball tractography study. AJNR Am J Neuroradiol 30:282–289.

Wakana S, Caprihan A, Panzenboeck MM, Fallon JH, Perry M, Gollub RL, et al. 2007. Reproducibility of quantitative tractography methods applied to cerebral white matter. Neuroimage 36:630–644.

Weeden VJ, Wang RP, Schmahmann JD, Benner T, Tseng WY, Dai G, et al. 2008. Diffusion spectrum magnetic resonance imaging (DSI) tractography of crossing fibers. Neuroimage 41:1267–1277.

Westerhausen R, Gruner R, Specht K, Hugdahl K. 2009. Functional relevance of interindividual differences in tempral lobe callosal pathways: a DTI tractography study. Cereb Cortex 19:1322–1329.

Westerhausen R, Kompus K, Dramsdahl M, Falkenberg LE, Gruner R, Hjelmervik H, Specht K, Plessen K, Hugdahl K. 2011. A critical re-examination of sexual dimorphism in the corpus callosum microstructure. Neuroimage 56:874–880.

Westerhausen R, Kreuder F, Dos Santos Sequeira S, Walter C, Woerner W, Wittling RA, et al. 2004. Effects of handedness and gender on macro- and microstructure of the corpus callosum and its subregions: a combined high-resolution and diffusion-tensor MRI study. Brain Res Cogn Brain Res 21:418–426.

Williams VJ, Juranek J, Stuebing K, Cirino PT, Dennis M, Fletcher J. 2013. Examination of frontal and parietal tectocortical attention pathways in spina bifida myelomeningocele using probabilistic diffusion tractography. Brain Connect 3:512–522.

Williams VJ, Juranek J, Stuebing KK, Cirino PT, Dennis M, Bowman RM, Blaser S, Kramer L, Fletcher J. 2015. Post-shunt lateral ventricular volume, white matter integrity, and intellectual outcomes in spina bifida and hydrocephalus. J Neurosurg Pediatr 15:410–419.

Witelson SF. 1985. The brain connection: the corpus callosum is larger in left-handers. Science 229:665–668.

Woolrich MW, Jbabdi S, Patenaude B, Chappell M, Makni S, Behrens TE, et al. 2009. Bayesian analysis of neuroimaging data in FSL. Neuroimage 45:173–186.

Address correspondence to:
Kailyn A. Bradley
Behavioral Science Unit
Pediatric Mood and Anxiety Disorders Program
Icahn School of Medicine at Mount Sinai
1240 Park Avenue
New York, NY 10029

E-mail: kailyn.bradley@gmail.com